Photonic crystal micropost as a microarray platform

Chih-Wei Chang and Cheng-Sheng Huang*

Department of Mechanical Engineering, National Chiao Tung University, 1001 Ta Hsueh Rd., Hsinchu, 30010, Taiwan

*csh@nctu.edu.tw

Abstract: This study demonstrates a photonic crystal micropost (PCMP) substrate for microarray applications. The substrate comprises an array of circular MPs with a PC on top of these MPs. This substrate enables biomolecule-containing droplets to form a composite contact upon deposition, thus allowing biomolecules to be attached on only the MPs, forming *spots*. When the device (PC) is excited on resonance, the electric field intensity is enhanced on only the top surface of the MPs. This enables the fluorescence intensities to be enhanced up to 5.50x; principally, this enhancement does not engender an increase in the background (intensity outside MP or spots) and noise intensities. The PCMP substrate enhances the spot intensity and minimizes the background intensity, enabling the detection of lower concentration analytes.

OCIS codes: (050.0050) Diffraction and gratings; (050.5298) Photonic crystals; (170.2520) Fluorescence microscopy.

References and links

1. D. J. Brennan, D. P. O'Connor, E. Rexhepaj, F. Ponten, and W. M. Gallagher, "Antibody-based proteomics: fast-tracking molecular diagnostics in oncology," Nat. Rev. Cancer **10**(9), 605–617 (2010).
2. H. Zhu and M. Snyder, "Protein chip technology," Curr. Opin. Chem. Biol. **7**(1), 55–63 (2003).
3. B. B. Haab, "Methods and applications of antibody microarrays in cancer research," Proteomics **3**(11), 2116–2122 (2003).
4. J. Glökler and P. Angenendt, "Protein and antibody microarray technology," J. Chromatogr. B Analyt. Technol. Biomed. Life Sci. **797**(1-2), 229–240 (2003).
5. E. A. Winzeler, M. Schena, and R. W. Davis, "Fluorescence-based expression monitoring using microarrays," Methods Enzymol. **306**, 3–18 (1999).
6. C. R. Sabanayagam and J. R. Lakowicz, "Increasing the sensitivity of DNA microarrays by metal-enhanced fluorescence using surface-bound silver nanoparticles," Nucleic Acids Res. **35**(2), e13 (2006).
7. R. A. Irizarry, D. Warren, F. Spencer, I. F. Kim, S. Biswal, B. C. Frank, E. Gabrielson, J. G. N. Garcia, J. Geoghegan, G. Germino, C. Griffin, S. C. Hilmer, E. Hoffman, A. E. Jedlicka, E. Kawasaki, F. Martínez-Murillo, L. Morsberger, H. Lee, D. Petersen, J. Quackenbush, A. Scott, M. Wilson, Y. Yang, S. Q. Ye, and W. Yu, "Multiple-laboratory comparison of microarray platforms," Nat. Methods **2**(5), 345–350 (2005).
8. Y. Fu and J. R. Lakowicz, "Enhanced fluorescence of Cy5-labeled DNA tethered to silver island films: fluorescence images and time-resolved studies using single-molecule spectroscopy," Anal. Chem. **78**(17), 6238–6245 (2006).
9. R. C. Zangar, S. M. Varnum, and N. Bollinger, "Studying cellular processes and detecting disease with protein microarrays," Drug Metab. Rev. **37**(3), 473–487 (2005).
10. R. C. Zangar, D. S. Daly, and A. M. White, "ELISA microarray technology as a high-throughput system for cancer biomarker validation," Expert Rev. Proteomics **3**(1), 37–44 (2006).
11. S. F. Kingsmore, "Multiplexed protein measurement: technologies and applications of protein and antibody arrays," Nat. Rev. Drug Discov. **5**(4), 310–321 (2006).
12. G. MacBeath and S. L. Schreiber, "Printing proteins as microarrays for high-throughput function determination," Science **289**(5485), 1760–1763 (2000).
13. B. Schweitzer, S. Wiltshire, J. Lambert, S. O'Malley, K. Kukanskis, Z. Zhu, S. F. Kingsmore, P. M. Lizardi, and D. C. Ward, "Immunoassays with rolling circle DNA amplification: A versatile platform for ultrasensitive antigen detection," Proc. Natl. Acad. Sci. U.S.A. **97**(18), 10113–10119 (2000).
14. W. Zhang, N. Ganesh, P. C. Mathias, and B. T. Cunningham, "Enhanced fluorescence on a photonic crystal surface incorporating nanorod structures," Small **4**(12), 2199–2203 (2008).
15. W. Hu, Y. Liu, H. Yang, X. Zhou, and C. M. Li, "ZnO nanorods-enhanced fluorescence for sensitive microarray detection of cancers in serum without additional reporter-amplification," Biosens. Bioelectron. **26**(8), 3683–3687 (2011).

#256865 Received 5 Jan 2016; revised 30 Jan 2016; accepted 30 Jan 2016; published 4 Feb 2016

16. S. Ricciardi, F. Frascella, A. Angelini, A. Lamberti, P. Munzert, L. Boarino, R. Rizzo, A. Tommasi, and E. Descrovi, "Optofluidic chip for surface wave-based fluorescence sensing," Sens. Actuators B **215**, 225–230 (2015).
17. E. Descrovi, F. Frascella, M. Ballarini, V. Moi, A. Lamberti, F. Michelotti, F. Giorgis, and C. F. Pirri, "Surface label-free sensing by means of a fluorescent multilayered photonic structure," Appl. Phys. Lett. **101**(13), 131105 (2012).
18. K. Toma, E. Descrovi, M. Toma, M. Ballarini, P. Mandracci, F. Giorgis, A. Mateescu, U. Jonas, W. Knoll, and J. Dostálek, "Bloch surface wave-enhanced fluorescence biosensor," Biosens. Bioelectron. **43**, 108–114 (2013).
19. K. Aslan, I. Gryczynski, J. Malicka, E. Matveeva, J. R. Lakowicz, and C. D. Geddes, "Metal-enhanced fluorescence: an emerging tool in biotechnology," Curr. Opin. Biotechnol. **16**(1), 55–62 (2005).
20. J. R. Lakowicz, C. D. Geddes, I. Gryczynski, J. Malicka, Z. Gryczynski, K. Aslan, J. Lukomska, E. Matveeva, J. Zhang, R. Badugu, and J. Huang, "Advances in surface-enhanced fluorescence," J. Fluoresc. **14**(4), 425–441 (2004).
21. T. Yamaguchi, T. Kaya, and H. Takei, "Characterization of cap-shaped silver particles for surface-enhanced fluorescence effects," Anal. Biochem. **364**(2), 171–179 (2007).
22. S. M. Tabakman, L. Lau, J. T. Robinson, J. Price, S. P. Sherlock, H. Wang, B. Zhang, Z. Chen, S. Tangsombatvisit, J. A. Jarrell, P. J. Utz, and H. Dai, "Plasmonic substrates for multiplexed protein microarrays with femtomolar sensitivity and broad dynamic range," Nat. Commun. **2**, 466 (2011).
23. J. R. Lakowicz, "Radiative decay engineering 5: metal-enhanced fluorescence and plasmon emission," Anal. Biochem. **337**(2), 171–194 (2005).
24. H.-Y. Wu, W. Zhang, P. C. Mathias, and B. T. Cunningham, "Magnification of photonic crystal fluorescence enhancement via TM resonance excitation and TE resonance extraction on a dielectric nanorod surface," Nanotechnology **21**(12), 125203 (2010).
25. N. Ganesh, W. Zhang, P. C. Mathias, E. Chow, J. A. N. T. Soares, V. Malyarchuk, A. D. Smith, and B. T. Cunningham, "Enhanced fluorescence emission from quantum dots on a photonic crystal surface," Nat. Nanotechnol. **2**(8), 515–520 (2007).
26. A. Pokhriyal, M. Lu, V. Chaudhery, C.-S. Huang, S. Schulz, and B. T. Cunningham, "Photonic crystal enhanced fluorescence using a quartz substrate to reduce limits of detection," Opt. Express **18**(24), 24793–24808 (2010).
27. N. Ganesh, P. C. Mathias, W. Zhang, and B. T. Cunningham, "Distance dependence of fluorescence enhancement from photonic crystal surfaces," J. Appl. Phys. **103**(8), 083104 (2008).
28. C. S. Huang, S. George, M. Lu, V. Chaudhery, R. Tan, R. C. Zangar, and B. T. Cunningham, "Application of photonic crystal enhanced fluorescence to cancer biomarker microarrays," Anal. Chem. **83**(4), 1425–1430 (2011).
29. P. C. Mathias, S. I. Jones, H.-Y. Wu, F. Yang, N. Ganesh, D. O. Gonzalez, G. Bollero, L. O. Vodkin, and B. T. Cunningham, "Improved sensitivity of DNA microarrays using photonic crystal enhanced fluorescence," Anal. Chem. **82**(16), 6854–6861 (2010).
30. P. C. Mathias, N. Ganesh, and B. T. Cunningham, "Application of photonic crystal enhanced fluorescence to a cytokine immunoassay," Anal. Chem. **80**(23), 9013–9020 (2008).
31. S. L. Seurynck-Servoss, A. M. White, C. L. Baird, K. D. Rodland, and R. C. Zangar, "Evaluation of surface chemistries for antibody microarrays," Anal. Biochem. **371**(1), 105–115 (2007).
32. E. W. Olle, J. Messamore, M. P. Deogracias, S. D. McClintock, T. D. Anderson, and K. J. Johnson, "Comparison of antibody array substrates and the use of glycerol to normalize spot morphology," Exp. Mol. Pathol. **79**(3), 206–209 (2005).
33. H. Chandra, P. J. Reddy, and S. Srivastava, "Protein microarrays and novel detection platforms," Expert Rev. Proteomics **8**(1), 61–79 (2011).
34. C. Preininger, U. Sauer, J. Dayteg, and R. Pichler, "Optimizing processing parameters for signal enhancement of oligonucleotide and protein arrays on ARChip Epoxy," Bioelectrochemistry **67**(2), 155–162 (2005).
35. F. Frederix, K. Bonroy, G. Reekmans, W. Laureyn, A. Campitelli, M. A. Abramov, W. Dehaen, and G. Maes, "Reduced nonspecific adsorption on covalently immobilized protein surfaces using poly(ethylene oxide) containing blocking agents," J. Biochem. Biophys. Methods **58**(1), 67–74 (2004).
36. A. B. D. Cassie and S. Baxter, "Wettability of porous surfaces," Trans. Faraday Soc. **40**, 546–550 (1944).
37. R. Magnusson and S. S. Wang, "New principle for optical filters," Appl. Phys. Lett. **61**(9), 1022–1024 (1992).
38. Z. Yoshimitsu, A. Nakajima, T. Watanabe, and K. Hashimoto, "Effects of surface structure on the hydrophobicity and sliding behavior of water droplets," Langmuir **18**(15), 5818–5822 (2002).
39. X. T. Zhang, M. Jin, Z. Y. Liu, D. A. Tryk, S. Nishimoto, T. Murakami, and A. Fujishima, "Superhydrophobic TiO2 surfaces: Preparation, photocatalytic wettability conversion, and superhydrophobic-superhydrophilic patterning," J. Phys. Chem. C **111**(39), 14521–14529 (2007).
40. N. A. Patankar, "On the modeling of hydrophobic contact angles on rough surfaces," Langmuir **19**(4), 1249–1253 (2003).
41. N. A. Patankar, "Transition between superhydrophobic states on rough surfaces," Langmuir **20**(17), 7097–7102 (2004).
42. R. N. Wenzel, "Resistance of solid surfaces to wetting by water," Ind. Eng. Chem. **28**(8), 988–994 (1936).
43. C. S. Huang, S. George, M. Lu, V. Chaudhery, R. Tan, R. C. Zangar, and B. T. Cunningham, "Application of photonic crystal enhanced fluorescence to cancer biomarker microarrays," Anal. Chem. **83**(4), 1425–1430 (2011).

#256865 Received 5 Jan 2016; revised 30 Jan 2016; accepted 30 Jan 2016; published 4 Feb 2016

1. Introduction

Protein microarray technology is crucial for detecting circulating biomarkers because it combines multiplexed detection, minimal reagent usage, and high sensitivity. Moreover, protein microarrays are valuable tools for investigating cellular protein production and protein–protein interaction networks, and they thus have potential applications as a clinical tool in disease diagnosis [1–4] and drug discovery [4].

Protein microarray assays are typically performed on planar surfaces, such as glass slides, upon which immobilized ligands selectively capture analytes from a test sample. Such assays can be easily multiplexed in a microarray format in which captured ligands are applied to the substrate in distinct microspots/spots (with a typical diameter ranging from 100 to 200 μm), enabling the detection of many analytes simultaneously [5–12]. Upon completion of the assays, a focused laser beam is scanned across the glass substrate to generate an image of fluorescence intensity output as a function of position. Despite the sensitivity afforded by this approach, the detection limit must be further improved to observe/quantify the analytes at lower concentrations.

Several techniques have been adopted in assay protocols to amplify the fluorescence output for enhancing the detection sensitivity and improving the limit of detection. These techniques can be classified into two approaches according to their mechanisms: chemical and physical. Chemical approaches include tyramide amplification (relying on reporter enzymes) [10] and rolling circle DNA amplification, which requires extensive chemical labeling of analytes with DNA primers [13]. Physical approaches entail exploring the possibility of using special substrates for enhancing the fluorescence intensity directly without any additional experimental steps or chemical reagents. Different micro/nanotextured substrates have been developed for increasing the overall surface area, thus increasing the density of capture ligands [14–18] to increase the fluorescence intensity. Fluorophore emission is proportional to the excitation electric field intensity. Hence, the metal enhanced fluorescence (MEF)-based electromagnetic amplification approach has attracted considerable attention in recent years because of its effectiveness in generating a localized enhanced electric field intensity through the coupling of external laser light source to surface plasmons [8, 19–22]. However, fluorophore emission quenching occurs for molecules within <10 nm [23] near metal surfaces, thus necessitating the use of a spacer layer, which might restrict the extensive adoption of MEF for practical applications. Recently, dielectric-based optical resonators of photonic crystal (PC) surfaces have been demonstrated to provide a considerably higher quality factor (Q, which is approximately 1000) than that of surface plasmons; therefore, they can provide higher electric field enhancement [24–26]. In particular, PC surfaces have been demonstrated to not quench fluorophores [27], enabling the easy adoption of PC surfaces for practical applications [28–30].

In microarray applications, the background signal concerning the fluorescence intensity outside spots is obtained from various nonspecific bindings among antigens, detection antibodies, and fluorescent dyes. The detection reaches its limit when the background signal is extremely high such that the spot cannot be distinguished from the background. To reduce the background signal, most studies have focused on optimizing surface chemistries [31–33] or different blocking reagents [34, 35] for reducing nonspecific binding and subsequent background signals.

Despite the effectiveness of various amplification techniques, the amplification of the background signal and noise is inevitable [26, 29, 30], which compromises the assay performance. This study presents a PC micropost (PCMP) substrate for enhancing fluorescence and simultaneously ensuring that the background signal remains unamplified. The PCMP substrate comprises an array of MPs with a PC on top of the MPs [Fig. 1]. The dimensions of the MPs were designed such that when a biomolecule-containing droplet is applied on a PCMP substrate, the droplet forms a composite contact [36], enabling the biomolecules to attach only to the PC [Fig. 1(b)]. After the completion of the assay, the fluorescence-tagged biomolecules exist only on top of the MPs; thus, each droplet can

#256865 Received 5 Jan 2016; revised 30 Jan 2016; accepted 30 Jan 2016; published 4 Feb 2016

simultaneously enable the biomolecules to be immobilized on multiple MPs, forming multiple *spots*. Because no PC structure exists outside the MPs/spots, when the PC is excited on resonance, the amplified electric field intensity exists on only the surface of the PC, enhancing only the spot intensity without increasing the background signal.

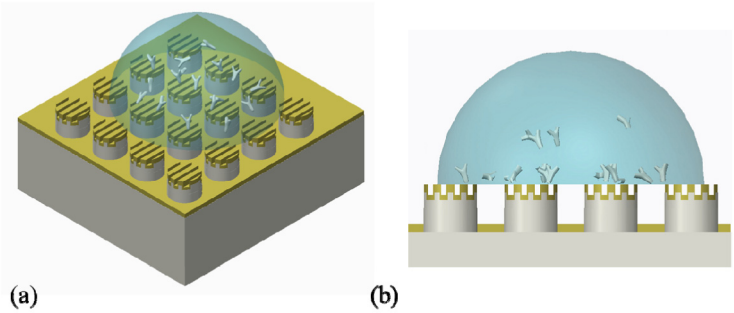

Fig. 1. (a) PCMP substrate with biomolecule-containing droplets. (b) Droplet forms composite contact enabling the biomolecules to be immobilized on only the top surface of MPs. The diameter, spacing and height of MPs are 60, 30 and 40 μm, respectively. The grating structure and MP are not to scale.

2. Material and methods

2.1 PC surface design

The PC used in this study (also known as guided-mode resonance [37])was a simple two-layer structure comprising a one-dimensional surface relief structure with a layer of high refractive index dielectric [Fig. 2]. When the incident wavelength and angle are appropriately combined, the external illumination can excite the device resonance [27], which supports optical standing waves confined in the high refractive index layer and extended to the surrounding media as an evanescent field. The near-field intensity associated with the evanescent field is strongly enhanced relative to the field intensity of the excitation light. The fluorescence intensity is proportional to the excitation intensity; therefore, the enhanced near field on the PC surface results in an amplified surface-bound fluorophore emission. The grating is formed on an ultraviolet (UV)-curable polymer (NOA68, n = 1.556, Norland Products Inc.) by using replica molding, which provides phase matching, allowing an external illumination to be coupled into the resonant modes. A high refractive index layer of TiO_2 (n = 2.22) is deposited on top of the grating to serve as a waveguiding layer supporting the resonant modes. In this study, the PC was designed for enhancing the emission of streptavidin-cyanine 5 (SA-Cy5), which is commonly used in fluorescence detection because of its strong quantum yield and high absorption efficiency at a HeNe laser wavelength of l = 632.8 nm.

To achieve a resonance at l = 632.8 nm, a commercial simulation tool (DiffractMOD, Rsoft Design Group) that is based on rigorous coupled-wave analysis was used in the design of the PC, resulting in a grating period, depth, and TiO_2 thickness of 400, 45, and 110 nm, respectively. In this design, the calculated transmission spectrum of the transverse magnetic (TM) mode has a wavelength range of 500–800 nm [Fig. 2(b)]. The transmission dip indicates that a resonant wavelength of 628 nm exists at normal incidence. Because of the surface chemistry layer and biomolecules attachment, the added thickness causes the resonant wavelength to shift by approximately 5 nm (based on our protocol). Hence, we intentionally designed a bare PC with a resonant wavelength at 628 nm.

#256865 Received 5 Jan 2016; revised 30 Jan 2016; accepted 30 Jan 2016; published 4 Feb 2016

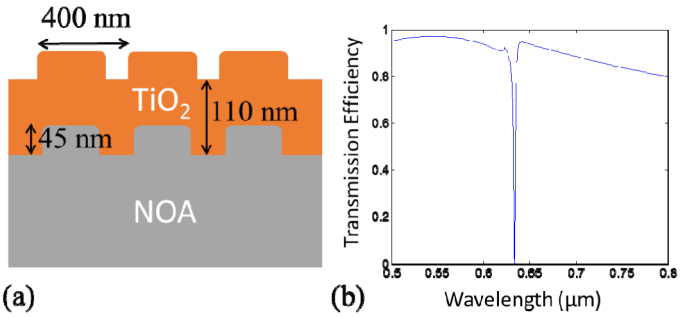

Fig. 2. (a) PC used in this study. The grating period, grating depth, and TiO_2 thickness are 400, 45, and 110 nm, respectively. (b) Simulated transmission spectrum of the TM mode showing the resonant wavelength at 628 nm.

2.2 MP design

The wettability of a surface by a droplet highly depends on the intrinsic chemical properties, surface energy, physical properties of the surface, and surface roughness [38–40]. Periodically patterned micro/nanostructured surfaces provide a convenient means of controlling the wettability by enabling the implementation of a well-defined surface roughness through a batch process of micro/nanofabrication [41]. The wettability of a solid surface is typically characterized by the apparent contact angle (CA). When the droplet size is much bigger than the size of the surface roughness, two models, namely Wenzel [42] and Cassie–Baxter models [36], are frequently used for predicting the CA and configuration of a droplet on a rough surface [41]. In the Wenzel model, the water droplets are in full contact with the rough surface (denoted as wetted contact). However, in the Cassie–Baxter model, the droplet is on top of only the rough surface and is in contact with solely the top surface as well as the air trapped between MPs (denoted as composite contact). To apply the capture ligands to each MP such that each MP forms a spot, the MP dimensions were designed according to the Cassie–Baxter model. Therefore, when a droplet containing capture ligands is applied on such a surface, the droplet forms a composite contact and the capture ligands can bind to only the surfaces of MPs [Fig. 1].

2.3 PCMP fabrication

Fabricating a PCMP substrate involves three main processes [Fig. 3]: 1. electron-beam (e-beam) lithography [Fig. 3(a)], 2. photolithography [Figs. 3(b) and 3(c)], and 3. replica molding [Figs. 3(d) and 3(e)] and film deposition [Fig. 3(f)].

First, grating patterns were fabricated on a Si wafer through e-beam lithography and reactive ion etching [Fig. 3(a)]. Subsequently, a thin layer (40 μm) of SU-8 2035 (negative photoresist, MicroChem Corp.) was spin-coated on top of the grating-patterned Si wafer. The wafer was soft-baked on a hotplate at 65 and 95 °C for 3 and 5.5 min, respectively. The SU-8 was then exposed through an I-line filter with a total energy of 75.4 mJ/cm^2 by using a contact aligner. For the postexposure bake, the film was placed on a hotplate at 65 and 95 °C for 1 and 5.5 min, respectively. The film was then developed in an SU-8 developer for 2.5 min with consistent agitation. Finally, to improve the structural strength for replica molding, the film was hard-baked at 150 °C for 15 min.

The next process involved replicating the grating and MP patterns simultaneously on a plastic substrate by using replica molding. To prevent permanent bonding between NOA68 and the sidewall of SU-8 and the bottom surface of Si, the SU-8/Si mold was silanized by exposing it to the vapor of (1H, 1H, 2H, 2H-perfluorooctyl) trichlorosilane (FOTS, Alfa Aesar) in a vacuum chamber for 30 min. An optical adhesive NOA68 was then sandwiched between the SU-8/Si master and a flexible sheet of polyethylene terephthalate (PET). In order to remove air bubbles, which can cause problems during replication, the device was put into

#256865 Received 5 Jan 2016; revised 30 Jan 2016; accepted 30 Jan 2016; published 4 Feb 2016

vacuum chamber at a pressure of 650 mmHg for 30 min. NOA68 was then cured by exposure to UV light (RC-742, Xenon); the polymer replica (PET/NOA68) was subsequently peeled of the SU-8/Si master. Next, a TiO_2 layer (110-nm thickness) was deposited on top of NOA68 through sputtering deposition.

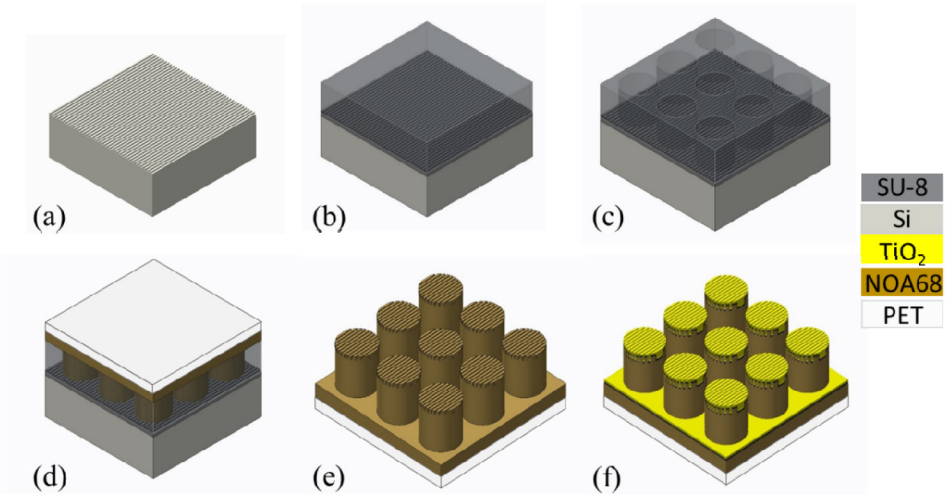

Fig. 3. PCMP fabrication process flow. (a) Si wafer with grating pattern using e-beam lithography. (b) Spin coating a layer of SU-8 2035. (c) Photolithography to pattern an array of holes. (d) Applying a UV-curable polymer in between a polyethylene terephthalate (PET) sheet and an SU-8 mold and then, curing through UV exposure. (e) Separating the UV polymer/PET from the Si/SU-8 mold. (f) Depositing a layer of TiO_2. The dimension of grating and MPs are not to scale.

2.4 Microarray spots

In this study, SA-Cy5 was used as a model fluorophore in the context of a microarray assay. To demonstrate the fluorescence enhancement and background minimization on a PCMP substrate, an MP substrate (without PC on top of the MPs) was used for comparison. Here, the MP substrate was fabricated using the processes illustrated in Figs. 3(c)–3(f), except that the substrate shown in Fig. 3(c) is a plain Si substrate, rather than a grating substrate used for PCMP fabrication.

To immobilize the SA-Cy5 on top of the PCMP and MP substrates, both substrates were silanized using FOTS as described. Subsequently, 4-µL droplets of SA-Cy5 in phosphate buffer saline (PBS) (at various concentrations: 50, 10, 2, 0.4, 0.08, and 0.016 µg/mL) were dispensed through a pipette on the MP and PCMP substrates. After incubation for 30 min in a humid chamber, both substrates were rinsed by immersion into PBS containing 0.05% Tween 20 (PBS-T) and deionized water for 3 minutes each to remove excess SA-Cy5 and then blow dried using N_2.

Fluorescence images were captured using a confocal microarray scanner (LS Reloaded, Tecan) equipped with a 633-nm laser and user-adjustable incident angle. The measured images were analyzed using image processing software called ImageJ, developed by National Institutes of Health, USA.

3. Results and discussion

The process flow developed in this study [Fig. 3] could effectively replicate a large area of an array of MPs with grating patterns simultaneously [Fig. 4]. The SEM images [Fig. 4(b)] indicate that the diameter and separation of the MPs are approximately equal to 60 and 30 µm, respectively. Moreover, the SEM [Figs. 4(c) and 4(d)] confirms that the grating period is

#256865 Received 5 Jan 2016; revised 30 Jan 2016; accepted 30 Jan 2016; published 4 Feb 2016

effectively replicated on top of the MPs; the grating period is 400 nm and duty cycle is 74%. The grating period accurately matches the designed dimension.

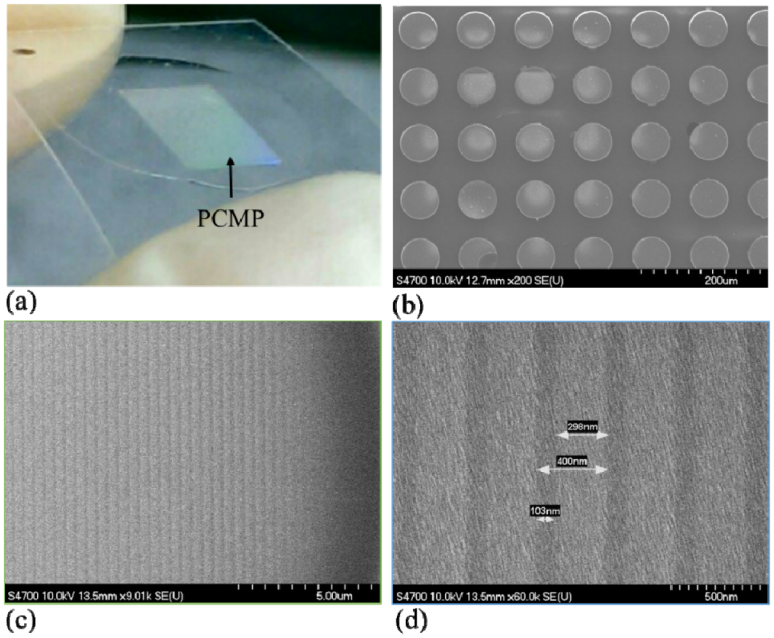

Fig. 4. (a) Plastic PCMP substrate with area of 0.6 × 0.8 cm. SEM images of the (b) top view of an array of MPs, (c) grating patterns on top of the MP, and (d) close-up view of grating patterns.

3.1 Composite contact

If a droplet forms a wetted contact with the MP substrate, then the biomolecule can attach to the sidewall of the MPs, which yields unwanted background. To minimize the background signal, a composite contact between a droplet and the MPs is preferred. To confirm that the fabricated MP can provide a composite contact, the PCMP was silanized using FOTS for 30 min, followed by sonication in solutions of toluene, methanol, and deionized water for 2 min each to remove excessive silane, and finally dried under a stream of N_2. Phosphate buffer saline (PBS) solution, a commonly used buffer solution in immunoassay, was employed to measure the CA. The CA measured (DSA100, KRUSS GmbH, Germany) using a 2-μL droplet of PBS dispensed on an unpatterned FOTS-coated surface was 87.6°. By contrast, it was approximately 135° on the MP FOTS-coated surface [Fig. 5]. The light passes through the gaps in the depression of the MPs, confirming the formation of a composite contact. For typical microarray spotter, the droplet is on the order of several nano liters resulting the printed spots of 100-200 μm. By reducing the dimension of microposts, it is possible the PCMP substrate can be worked with the current microarray spotter.

#256865 Received 5 Jan 2016; revised 30 Jan 2016; accepted 30 Jan 2016; published 4 Feb 2016

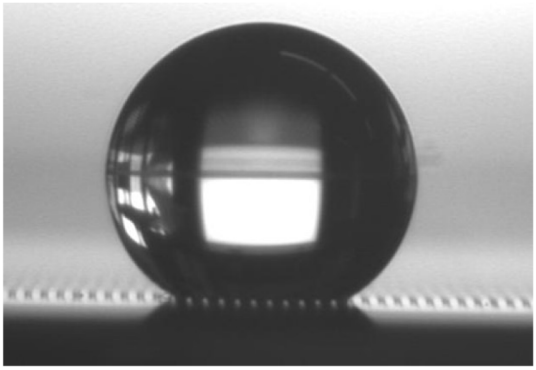

Fig. 5. Droplet forms a composite contact on a FOTS-coated PCMP surface.

3.2 Fluorescence image

Fluorescence images [Fig. 6] of a droplet of 50 μg/mL SA-Cy5 on PCMP and MP substrates were obtained using identical settings in a Tecan scanner with a resolution of 4 μm. Despite the observation of several missing spots engendered by incomplete or broken MPs during molding and separation, the fluorescent intensities obtained from the PCMP substrate can be enhanced compared with those obtained from the MP substrate. Moreover, when the designed MP dimensions are used, with only one droplet, multiple spots can be created simultaneously for microarray assay applications. A stronger vacuum pump or prolonged duration at vacuum step can be used to improve the replication of microposts.

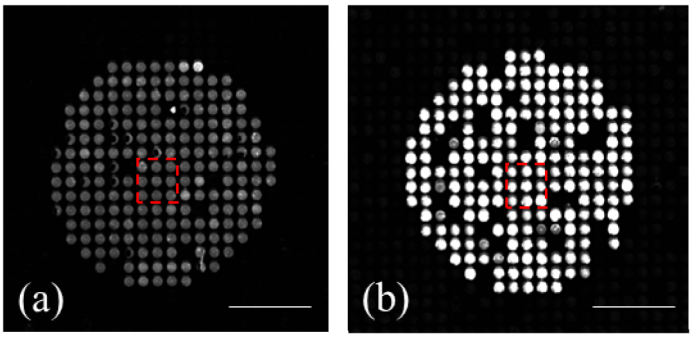

Fig. 6. Fluorescence images of a droplet of 50 μg/mL SA-Cy5 on (a) MP substrate and (b) PCMP substrate. The scale bar represents 500 μm.

A portion comprising nine spots was selected for the spot and background signal intensity analysis. Figures 7(a) and 7(b) depicts fluorescence images for the PCMP and MP substrates for six concentrations of SA-Cy5 and one blank solution containing only PBS. The effect on fluorescence enhancement can be observed in Fig. 7(c), where the intensities of the pixels along the dashed line were generated for concentrations of 10 and 0.4 μg/mL. The average spot intensities for a concentration of 10 μg/mL were approximately 5163 and 1698 cts for the PCMP and MP substrates, respectively. For a concentration of 0.4 μg/mL, the signal intensities on the PCMP and MP substrates were 723 and 158 cts, respectively. The signal intensity between spots (referred to as background intensity) was in the range 40–60 cts, in which no significant difference existed between the PCMP and MP substrates.

#256865 Received 5 Jan 2016; revised 30 Jan 2016; accepted 30 Jan 2016; published 4 Feb 2016

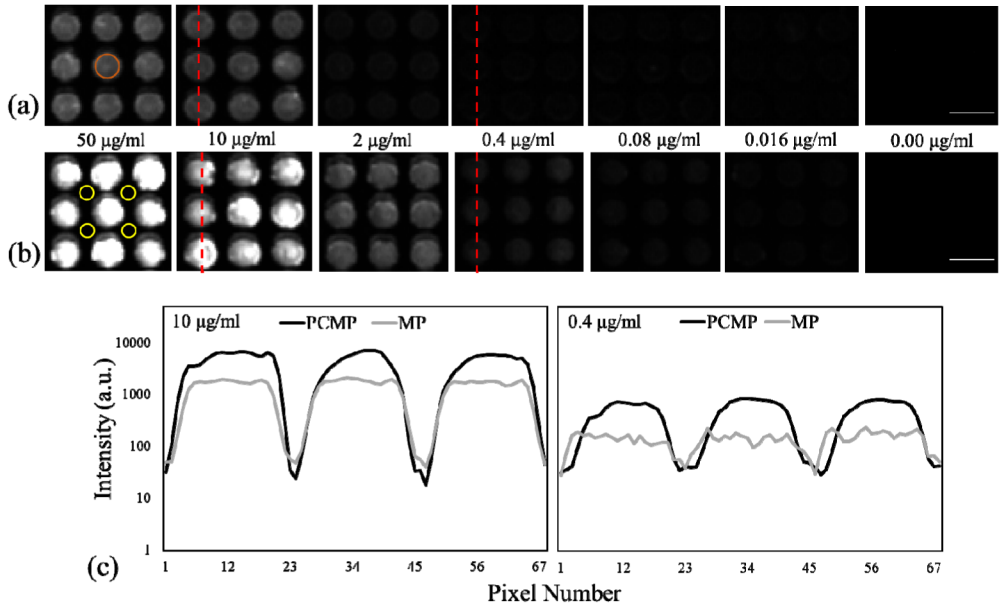

Fig. 7. Fluorescence images at various concentrations of SA-Cy5 on (a) MP and (b) PCMP substrates. The orange and yellow circles indicate the spot and background intensities as described in the text. (c) The line profiles at three spots for MP and PCMP substrates at 10 and 0.4 μg/mL. The scale bar represents 100 μm.

3.3 Spot and background intensity analysis

To accurately quantify the fluorescence intensity of each spot, ImageJ was used. A circle with a diameter of 60 μm was overlaid on top of a spot and the average intensity of each pixel within the circle was designated to the spot intensity. The mean intensity and standard deviation of nine spots was then calculated.

As mentioned, current fluorescence enhancement techniques always result in background signal enhancement. A background signal was defined as the fluorescence intensity outside the spots. To obtain the background signal, a circle with a diameter of 30 μm was overlaid on the region between the MPs/spots, and the average intensity of each pixel within the circle was used to represent the background intensity of that region. The first image in Fig. 7(b) shows the intensity at four yellow circles, which can then be calculated and designated as the background intensity for a specific SA-Cy5 concentration. Table 1 and Fig. 8 show a summary of the measured spot and background intensity with their corresponding standard deviations for the PCMP and MP substrates. The spot intensity was enhanced through the resonant mode excited in the PC structure on top of the MPs whose enhancement factor was defined as the spot intensity of PCMP divided by the spot intensity of MP and was in the range 1.31x–5.50x depending on the concentration.

The background intensities at different concentrations were between 42 ± 4 and 58 ± 10 and 40 ± 1 and 54 ± 2 for the MP and PCMP substrates, respectively. The slight variation in both background signals is probably due to the device or experimental variations. These results demonstrate that in contrast to the substrates used previously [30, 43], the PCMP substrate eliminates the amplification of background signals obtained through different fluorescence enhancement techniques, and only the spot intensity is amplified. The background signal was minimized through three possible mechanisms: (a) elimination of nonspecific binding in the area outside the MPs/spots because of composite contact, (b) selection of the focal plane on top of the MPs during fluorescent image scanning, and (c) the absence of an excitation-field-enhancing PC outside the spot.

#256865 Received 5 Jan 2016; revised 30 Jan 2016; accepted 30 Jan 2016; published 4 Feb 2016

3.4 Sensitivity and resolution

Sensitivity is defined as the change in the output signal for a given change in the concentration. Within the concentration range used in this study, the sensitivity was nonlinear for both substrates; however, Fig. 8 clearly demonstrates that the PCMP exhibits higher sensitivity because the PC enhances fluorescence as indicated by the steeper curve, which is consistent with the results of previous studies [28, 30]. For a lower concentration range (0.016–0.4 μg/mL), the relationship between the intensity and the concentration was fairly linear [Fig. 8(b)]. The sensitivity was 1235 fluorescence intensity/(μg/mL) from the PCMP substrate, as opposed to 82 fluorescence intensity/(μg/mL) from the MP substrate, resulting in 15-fold enhancement. The higher sensitivity (marked change in the output for a given change in the concentration) enables the PCMP to detect small changes in the concentration more accurately.

The increase in sensitivity is compromised if the resolution is inversely affected. The resolution can be calculated as three times the noise divided by the sensitivity, which represents the smallest change in concentrations that can be distinguished from noise. For example, for 0.4 μg/mL SA-Cy5, the resolutions are 0.55 and 0.23 μg/mL for the MP and PCMP substrates, respectively, representing a 58.4% reduction (improvement) in the resolution for the PCMP substrate. For 0.08 and 0.016 μg/mL SA-Cy5, similar resolution improvement trends can be obtained, where the resolutions on the PCMP and MP substrates are improved by 74.5% and 80.8%, respectively.

Table 1. Measured spot and background intensities at different SA-Cy5 concentrations obtained from the MP and PCMP substrates.

SA-Cy5 Concentration (μg/ml)		50	10	2	0.4	0.08	0.016	0
MP Intensity (a.u.)	Spot	3300 ± 194	1698 ± 208	422 ± 29	158 ± 15	138 ± 13	123 ± 10	46 ± 2
	Background	57 ± 4	50 ± 2	45 ± 1	57 ± 12	58 ± 10	53 ± 12	42 ± 4
PCMP Intensity (a.u.)	Spot	14940 ± 1851	5163 ± 954	2322 ± 140	723 ± 94	357 ± 50	232 ± 29	71 ± 5
	Background	48 ± 4	40 ± 1	42 ± 2	44 ± 3	43 ± 3	46 ± 2	54 ± 2
Enhancement Factor		4.53	3.04	5.50	4.59	2.60	1.88	1.31

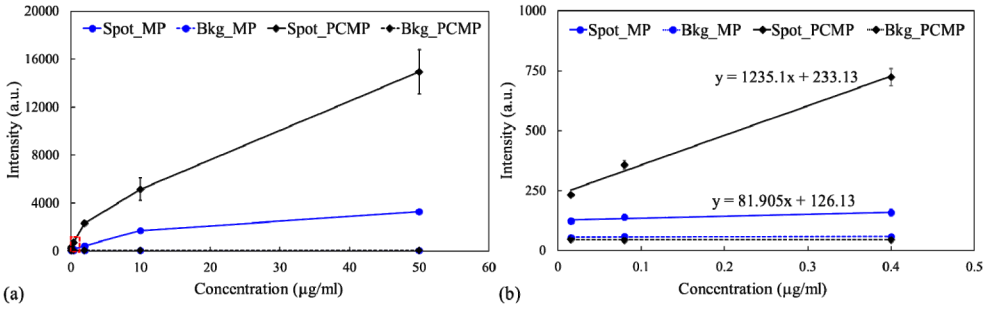

Fig. 8. (a) Spot and background intensities at different SA-Cy5 concentrations on the PCMP and MP substrates. (b) The data from (a) of the three lowest SA-Cy5 concentrations. The sensitivities were calculated as the slopes of the linearly fitted curves for the PCMP and MP substrates.

4. Conclusion

The ability to detect weak fluorescent signals above the background noise (mainly from autofluorescence and nonspecific binding) is particularly crucial for identifying biomolecular

#256865 Received 5 Jan 2016; revised 30 Jan 2016; accepted 30 Jan 2016; published 4 Feb 2016

analytes present at extremely low concentrations. In this study, we demonstrate a PCMP substrate, which can offer numerous considerable improvements over current technologies by combining the following mechanisms. Currently, a serial printing method is generally used to prepare microarray capture ligands in which each droplet corresponds to a spot. When a PCMP substrate with appropriate dimensions in MPs, is used, multiple replicates can be created simultaneously through composite contact with a single droplet. Microarray spotters create spots with a diameter of approximately 100–200 μm because of the size limitation of a piezoelectric dispenser or quill pin. When the PCMP substrate is used, the diameter of the MP can be easily reduced to less than 10 μm. Similarly, the diameters of the microarray spots can be easily reduced to below 10 μm, which can increase the array densities. By incorporating PC structures on the MPs, we can operate at the PC's resonance to amplify the electric field intensity at the surface; therefore, enhancing the fluorescence emission results in higher sensitivity and resolution. In particular, the PCMP substrate does not involve the amplification of the background and noise intensities.

Acknowledgments

This research was supported by the Ministry of Science and Technology, Taiwan (Grant No. 103-2221-E-009-075). The authors thank Genomics Core Facility, Institute of Molecular Biology, Academia Sinica; Nano Facility Center, National Chiao Tung University; and National Nano Device Laboratories, Taiwan, for supporting the fluorescence measurement and PCMP fabrication and characterization.

#256865 Received 5 Jan 2016; revised 30 Jan 2016; accepted 30 Jan 2016; published 4 Feb 2016